

## Laboratory for Organic Optics and Electronics

### Academic and Research Staff

Prof. T. Akinwande, Prof. M. Baldo, Prof. M. Bawendi, Prof. V. Bulovic, Jianglong (Gerry) Chen, Conor Madigan, Matthew Panzer, Prof. M. Schmidt, Prof. C.G. Sodini, Prof. T. Swager, Jonathan (Yaakov) Tischler, Burag Yaglioglu

### Visiting Scientists and Research Affiliates

P. Benning (HP), T. Bloomstein (Lincoln Laboratory), M. Chaparala (HP), F. Jaworski (Raytheon), P. Mardilovich (HP), A. Nurmikko (Brown Univ.), D. Schut (HP)

### Graduate Students

H. Abdu, G. Akselrod, P. Anikeeva, A. Arango, S. Bradley, D. Friend, J. Ho, Q. Hu, J. Leu, I. Nausieda, T. Osedach, S. Paydavosi, J. Rowehl, Y. Shirasaki, H. Tang, V. Wood, J. Yu

### Technical and Support Staff

L. Kim, Asst.  
M. Pegis, Admin. Asst.

## 1. Stability of Metal Oxide-based Field-effect Transistors

### Sponsors

Hewlett-Packard, DARPA

### Project Staff

B.Yaglioglu, A.Wang, K. Ryu, H. Tang, C.G. Sodini, A.I. Akinwande, V. Bulović

Over the last few years, there has been a considerable effort to understand the behavior of metal-oxide-channel field-effect transistors (FETs) in order to produce devices for low-cost, large-area electronic applications [1-3]. Field-effect mobility, sub-threshold slope, and threshold voltage of FETs are the main parameters that need to be characterized to design circuits made of amorphous oxide semiconductors. Just as important as these characteristics is the endurance of FETs over repeated switching cycles, which determines the reliability of the transistors.

In this study we test the stability of FETs that have a polymer dielectric, parylene, and an oxide semiconductor (ZnO:In<sub>2</sub>O<sub>3</sub>). The devices are processed lithographically at low temperatures ( $T \leq 100$  °C). Figure 1 shows transfer characteristics that are obtained by repetition of current-voltage (I-V) sweeps under a gate bias between measurements. Preliminary results of I-V tests along with capacitance-voltage (C-V) measurements (see Figure 2) show a positive shift in the threshold voltage. Two possible mechanisms that are originally proposed for similar shifts in amorphous Si FET's are metastable state generation in the semiconductor and charge trapping in the dielectric [4]. Operation of stability experiments at different temperatures and bias gate voltages are conducted to elucidate the instability mechanisms in these hybrid (inorganic/organic) devices. The outcome of these experiments will provide a path for increasing the performance and lifetime of transistors based on oxide semiconductors.

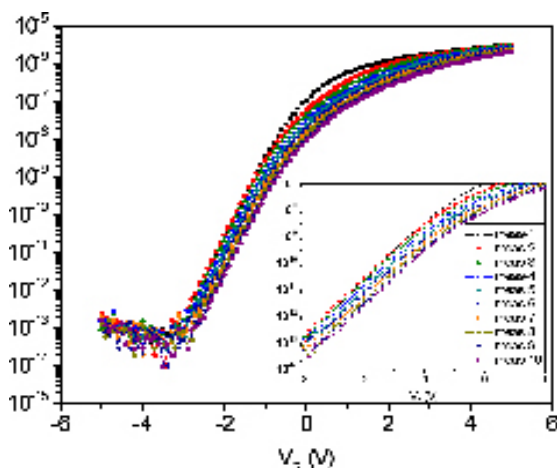


**Figure 1:** Transfer characteristics of a transistor under a bias stress,  $V_{GS} = 10V$  and  $V_{DS} = 0V$ , between measurements (stress time = 20s). Data are taken from -5V to 5V with 0.1V steps while  $V_{DS} = 1V$ . The sub-threshold regime of curves is enlarged in the inset.

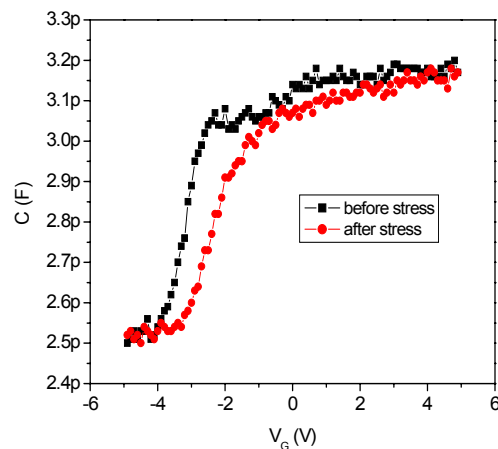


**Figure 2:** Quasi-static C-V measurements collected from the same device before and after bias stress test.

### References

- [1] P.F. Carcia, R.S McLean, M.H. Reilly, and G. Nunes, "Transparent ZnO thin film transistors fabricated by rf magnetron sputtering," *Applied Physics Letters*, vol. 82, no. 7, pp. 1117-1119, Feb. 2003.
- [2] N.L. Dehuff, E.S. Kettenring, D. Hong, H.Q. Chiang, J.F. Wager, R.L. Hoffman, C.H. Park, and D.A. Keszler, "Transparent thin film transistors with zinc indium oxide channel layer," *Journal of Applied Physics*, vol. 97, no. 6, pp. 064505:1-5, Mar. 2005.

[3] H. Kumomi, K. Nomura, T. Kamiya, and H. Hosono, "Amorphous oxide channel TFTs," *Thin Solid Films*, vol. 516, no. 7, pp.1516-1522, Feb. 2008.

[4] M.J. Powell, C. van Berkel, and J R. Hughes, "Time and temperature dependence of instability mechanisms in amorphous silicon thin-film transistors," *Applied Physics Letters*, vol. 54, no. 14, pp. 1323-1325, Jan. 1989.

## 2. Organic Floating-gate Memory Devices

### Sponsors

SRC/FCRP MSD

### Project Staff

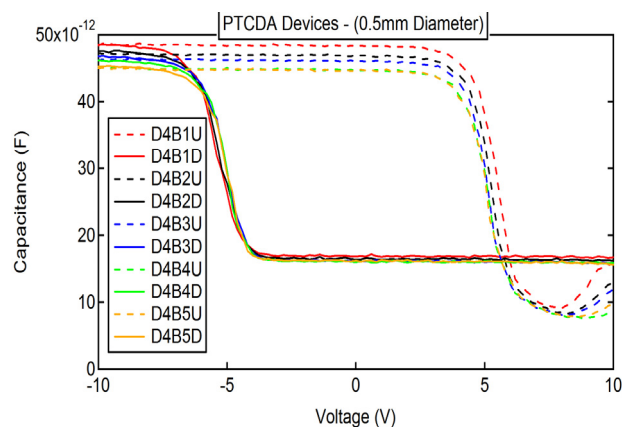
H. Abdu, S. Paydavosi, O.M. Nayfeh, D.A. Antoniadis, V. Bulović

Conventional non-volatile flash memories face obstacles to continued scaling, such as the inability to use thinner tunneling oxides and poor charge retention due to defects in the tunneling oxide [1]. A possible solution is to replace the continuous floating gate, where the charge is stored, with a segmented charge storage film, so that defects in the structure would affect only a few of the many segments that comprise the floating gate [2]. From our earlier work on nanocrystal thin films as floating gates, we established the need for the smallest possible segmented structures, which led us to the use of organic films as floating gates in non-volatile flash memories. As an example, a single organic molecule of 3,4,9,10 -parylene tetracarboxylic dianhydride (PTCDA) occupies 1 nm<sup>2</sup> in area and is capable of storing and retaining a single charge. A thin film of PTCDA molecules would therefore provide 10<sup>14</sup> distinct charge storage sites per cm<sup>2</sup>, a remarkably high number of storage sites, even when we take into account the fact that only a few percent of these would be occupied when the floating gate is charged. If a defect were present in the tunneling oxide below the floating gate, only a few discreet molecules of PTCDA would be affected due to poor lateral conduction between PTCDA molecules. We can, therefore, project that such a molecular thin film of PTCDA is likely to meet the demanding size and packing density requirements of the advancing flash memory technology.

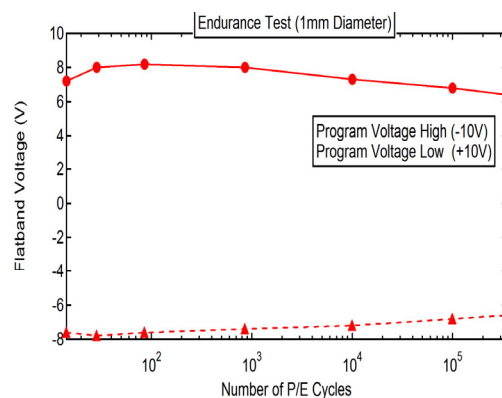
To demonstrate charge retention in an organic thin film, we construct an organic floating gate capacitor, shown in Figure 2 (inset), by depositing 4 nm of PTCDA as the floating gate. As for the gate dielectric, SiO<sub>2</sub> was deposited using Plasma Enhanced CVD (PECVD), which allowed for low temperature oxidation and minimal damage to the organic film below. This capacitor structure is a first step to demonstrating a floating-gate memory cell, as it proves significant in understanding the organic molecular film's ability to be written (charged), erased (discharged), and read (retain charge).

Figure 1 demonstrates the functionality of the organic floating gate capacitor. The capacitance voltage (C-V) plot exhibits hysteresis, which indicates the flatband voltage shift that exists due to charge storage. Also, as Figure 2 shows, the device performs well in endurance tests, withstanding over 300,000 program/erase cycles without much deterioration in the flatband voltage shift.

This initial set of data signifies the potential for organic floating-gate memories as an advancement of flash memory devices. With the scaling enabled by the nano-segmented molecular floating gate, this technology has the potential to achieve higher memory density, decreased power consumption, and increased read/write/erase speeds, all of which are important benchmarks for future non-volatile memory devices [3].



**Figure 1:** C-V plot of several organic floating-gate capacitors with characteristic hysteresis. Electron charging at -10V and hole charging at +10V.



**Figure 2:** Schematic diagram of an organic floating-gate capacitor (subset). Endurance test demonstrating over 300,000 program/erase cycles without significant loss in device performance.

### References

- [1] K. Kinam, "Technology for sub-50nm DRAM and NAND flash manufacturing," *International Electronic Devices Meeting*, 1609340, pp. 323-326, Dec. 2005.
- [2] O. Nayfeh, D. Antoniadis, K. Mantey, and M. Nayfeh, "Memory effects in metal-oxide-semiconductor capacitors incorporating dispersed highly monodisperse 1-nm silicon nanoparticles," *Applied Physics Letters*, vol. 90, p. 153105, 2007.
- [3] P. Pavan, R. Bez, P. Olivo, and E. Zanoni, "Flash memory cells--an overview," *Proc. IEEE*, vol. 85, no. 8, Aug. 2007, pp. 1248-1271.

### 3. Inkjet-printed Quantum Dot and Polymer Composites for AC-driven Electroluminescent Devices

#### Sponsors

ISN, PECASE, NDSEG

#### Project Staff

V. Wood, J. Chen, M.J. Panzer, M.S. Bradley, J.E. Halpert, M.G. Bawendi, V. Bulović

We introduce a technique for the reliable deposition of intricate, multicolored patterns using a quantum dot (QD) and polymer composite and demonstrate its application for robust AC-driven displays with high brightness and saturated colors. The AC electroluminescent (AC EL) devices are a well-established technology [1]. Their relatively simple fabrication and long operating lifetimes make them desirable for large-area displays; however, a major challenge with AC EL remains finding efficient and stable red phosphors for multicolored displays. Colloidally synthesized QDs are robust, solution-processable lumophores offering tunable and narrowband photoluminescence across the visible spectrum [2]. By integrating QDs into an AC EL device, we demonstrate patterning of saturated red, green, and blue pixels that operate at video brightness.

The concept behind the device operation is optical downconversion: red and green QDs absorb blue electroluminescence from phosphor grains and then emit at longer wavelengths. The device, pictured schematically in Figure 1, is fabricated with a layer-by-layer approach that is compatible with flexible substrates. A QD and polyisobutylene (PIB) solution is printed on conductive indium tin oxide (ITO) using a Hewlett Packard Thermal Inkjet Pico-fluidic dispensing system (TIPs). Figure 2a shows examples of the

intricate and multicolored patterns possible. The electroluminescent phosphor paste (ZnS:Cu powder in a transparent binder from Osram-Sylvania) is deposited uniformly over the sample using a disposable mask and doctor-blading to define the device area. Top contacts are made with conductive tape from 3M. This basic device structure is assembled and tested entirely under atmospheric conditions.

When an AC voltage waveform is applied across the device, we measure spectrally pure QD emission in the red and green and  $\sim 100$  Cd/m<sup>2</sup> brightness. Photographs of the red, green, and blue pixels of a working, AC-driven device appear in Figure 2b. The Commission International d'Eclairage (CIE) coordinates of the pixels device define a color triangle that is comparable to the International Telecommunication Union HDTV standard.

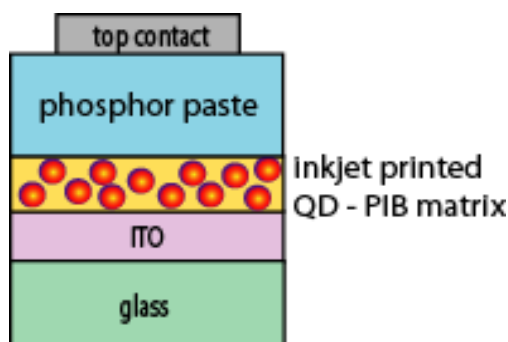


**Figure 1:** Schematic showing basic device structure.

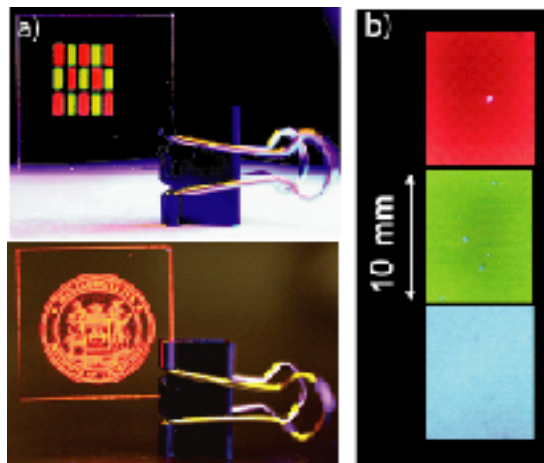


**Figure 2:** Photographs of a) photoluminescence of QD-PIB composites inkjet-printed on 1 in. x 1 in. indium tin oxide coated glass slides and b) emission from blue, green, and red pixels of completed devices driven at 70 V<sub>rms</sub> and 50 kHz.

## References

- [1] Y.A. Ono, *Electroluminescent Displays*. Singapore: World Scientific, 2000.
- [2] C.B. Murray, D.J. Norris, and M.G. Bawendi, "Synthesis and characterization of nearly monodispersed CdE (E= S, Se, Te) semiconductor nanocrystallites," *Journal of the American Chemical Society*, vol. 115, pp. 8706-8715, 1993.

#### 4. Exciton-polaritons at Room Temperature in Metal-dielectric Microcavities

##### Sponsors

DARPA, NDSEG, MIT NSF MRSEC

##### Project Staff

J.R. Tischler, M.S. Bradley, Y. Shirasaki, V. Bulović

Exciton-polariton-based photonic devices are a novel platform for realizing low-threshold lasing [1] and optical switching [2] in a scalable integrated architecture. Use of organic materials such as the excitonic component facilitates room-temperature operation of such devices [3]. Here we report room-temperature exciton-polariton devices consisting of layer-by-layer (LBL) assembled thin films of polyelectrolyte and the J-aggregates of the cyanine dye TDBC inserted in a resonantly-tuned planar  $\lambda/2n$  optical microcavity with metal mirror and dielectric Bragg reflector (DBR). The device exhibits Rabi-splitting of  $\Omega R = 125 \pm 7$  meV with a polyelectrolyte/J-aggregate layer that is only  $5.1 \pm 0.5$  nm thick [4]. Furthermore, the linewidth of the lower energy polariton state, measured on resonance, is  $\Gamma = 12.1$  meV. The ratio  $\Omega R/2\Gamma = 5.1$  indicates that the device operates in a limit where the light-matter coupling ( $\Omega R$ ) significantly exceeds competing dephasing processes ( $\Gamma$ ). These figures of merit are achieved by virtue of the nanostructured film's large absorption coefficient of  $\alpha \sim 1.0 \times 10^6$  cm<sup>-1</sup> and by location of the  $5.1 \pm 0.5$ -nm-thick layer at the microcavity anti-node. Rabi-splitting and polaritonic dispersion are observed in the reflectance, transmittance, and photoluminescence measurements of the device. Because strong coupling is achieved with such thin films, the majority of the microcavity modal volume is available for integrating a variety of optically active materials, such as colloidal quantum dots and fluorescent polymers, into devices that could leverage the coherent properties of the strongly coupled states. Moreover, the LBL process provides nanometer-scale thickness control of  $\sim 1.7$  nm per polymer/dye bi-layer, suggesting that this device can be used to investigate fundamental physical phenomena such as non-radiative energy transfer and laser action in the strong coupling limit.

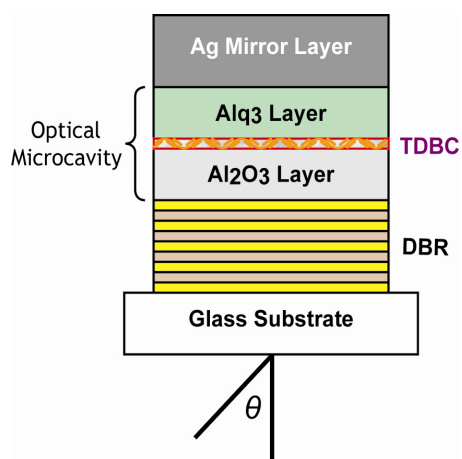


**Figure 1:** Device design of polaritonic structure. Microcavity consists of a DBR and a silver mirror layer. On top of the J-aggregate layer, a film of small molecule Alq3 is thermally evaporated.

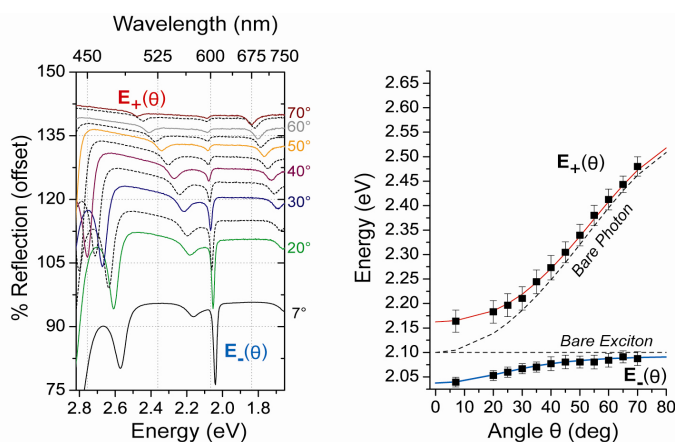


**Figure 2:** (a) Angularly resolved reflectance measurements and (b) dispersion relation for resonantly tuned polaritonic structure. The microcavity is resonantly tuned at normal (at  $\theta = 0^\circ$ ) to the exciton resonance of 2.10 eV. The  $E_-(\theta)$  denotes the lower energy polariton states;  $E_+(\theta)$ , the higher energy polariton states. Reflectance is measured with TE polarized incident light. Measurements from  $\theta = 20^\circ$  to  $70^\circ$  are relative values. Data at  $\theta = 7^\circ$  is absolute reflectance.

**References**

- [1] S. Christopoulos, G.B. von Hagersthal, A.J. Grundy, P. Lagoudakis, A.V. Kavokin, J.J. Baumberg, G. Christmann, R. Butte, E. Feltn, J.F. Carlin, and N. Grandjean, "Room-temperature polariton lasing in semiconductor microcavities," *Physical Review Letters*, vol. 98, pp. 126405:1-4, Mar. 2007.
- [2] N.A. Gippius, I.A. Shelykh, D.D. Solnyshkov, S.S. Gavrilov, Y.G. Rubo, A.V. Kavokin, S.G. Tikhodeev, and G. Malpuech, "Polarization multistability of cavity polaritons," *Physical Review Letters*, vol. 98, pp. 236401:1-4, June 2007.
- [3] D.G. Lidzey, D.D.C. Bradley, M.S. Skolnick, T. Virgili, S. Walker, and D.M. Whittaker, "Strong exciton-photon coupling in an organic semiconductor microcavity," *Nature*, vol. 395, no. 6697, pp. 53-55, Sept. 1998.
- [4] M.S. Bradley, J.R. Tischler, and V. Bulović, "Layer-by-layer J-aggregate thin films with a peak absorption constant of  $10^6 \text{ cm}^{-1}$ ," *Advanced Materials*, vol. 17, no. 15, pp. 1881-1886, Aug. 2005.

**5. Near-infrared J-aggregates for Exciton-polariton Optoelectronics****Sponsors**

ISN, NDSEG, MIT NSF MRSEC

**Project Staff**

M.S. Bradley, J.R. Tischler, Y. Shirasaki, V. Bulović

Thin films of J-aggregates of cyanine dyes, which found wide use in the 20th century in the photographic film industry, exhibit narrow linewidth and large oscillator strength, enabling their use in the first room-temperature solid-state electroluminescent devices that exhibit the strong-coupling regime of Cavity Quantum Electrodynamics (Cavity QED) [1]. As we demonstrated in a recent study, layer-by-layer (LBL)-assembled J-aggregate thin films can be precisely deposited in a specific location in a microcavity and contain a high density of aggregates, contributing to the observation of a peak thin-film absorption coefficient of  $1.05 \pm 0.1 \times 10^6 \text{ cm}^{-1}$ , among the highest ever measured for a neat thin film [2]. A recent study utilizing J-aggregates with exciton resonance in the near-infrared (NIR) spectral region demonstrated devices exhibiting strong coupling [3]. However, the J-aggregate films used were deposited by spin-coating, which results in inhomogeneous, thick films. In this work, we utilize the LBL deposition method to deposit thin films of these NIR J-aggregates, showing the same nanoscale thickness control and large peak thin-film absorption constant as observed in our previous studies for J-aggregates in the visible spectral region.

For deposition of thin films of NIR J-aggregates, substrates undergo sequential immersions in cationic and anionic solutions (SICAS). The cationic solution contains the very-low-molecular-weight polyelectrolyte PDAC (poly(dimethyldiallylammonium chloride)), and the anionic solution consists of the J-aggregating dye U3 (3-[[[(2Z)-5-chloro-2-[[[(3E)-3-[[[5-chloro-3-(3-triethylammonium-sulfonatopropyl)-1,3-benzothiazol-3-ium-2-yl]methylene]-2,5,5-trimethylcyclohex-1-en-1-yl) methylene]-1,3-benzothiazol-3(2H)-yl] propane-1-sulfonate). Figure 1 shows the reflectivity for films on glass substrates that underwent various numbers of SICAS, showing the NIR J-aggregate peak around  $\lambda=790 \text{ nm}$ , as observed in [3] for spin-coated films. Figure 2 shows an atomic force microscopy (AFM) image of the 6.5 SICAS film, which demonstrates the remarkably-low (XYZ nm) roughness of films produced using this technique, which will allow for incorporation of these films into optical microcavities without contributing to significant inhomogeneous broadening of the cavity resonance, as needed for development of strongly-coupled Cavity QED devices.

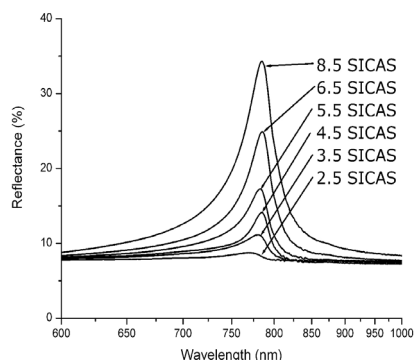


**Figure 1:** Reflectance of thin films of NIR J-aggregates deposited on glass substrates using the LBL deposition method.

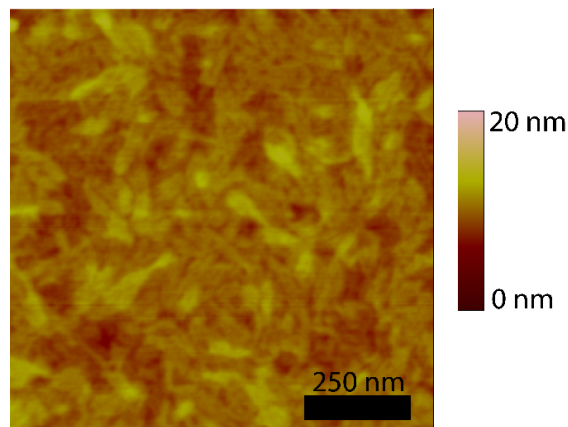


**Figure 2:** AFM image of the 6.5 SICAS film from Figure 1. The low roughness allows incorporation of these films into microcavities without significantly increasing the inhomogeneous linewidth of the cavity resonance.

## References

- [1] J.R. Tischler, M.S. Bradley, V. Bulović, J.H. Song, and A. Nurmikko, "Strong coupling in a microcavity LED," *Physics Review Letters*, vol. 95, no. 3, pp. 036401-036404, 2005.
- [2] M.S. Bradley, J.R. Tischler, and V. Bulović, "Layer-by-layer J-aggregate thin films with a peak absorption constant of  $10^6 \text{ cm}^{-1}$ ," *Advanced Materials*, vol. 17, no. 15, pp. 1881-1886, 2005.
- [3] J. Wenus, S. Ceccarelli, D.G. Lidzey, A.I. Tolmachev, J.L. Slominskii, and J.L. Bricks, "Optical strong coupling in microcavities containing J-aggregates absorbing in near-infrared spectral range," *Organic Electronics*, vol. 8, pp. 120-126, 2007.

## 6. Micro-patterning Organic Thin Films via Contact Stamp Lift-off for Organic Light-emitting Device Arrays

### Sponsors

CMSE, PECASE

### Project Staff

J. Yu, V. Bulović

Patterning of organics in electronic devices is done primarily by techniques that are limited in resolution or scalability or are potentially damaging to the organic material. We demonstrate a simple subtractive stamping technique for patterning micron-sized features on organic thin films of nanometer-range thickness. Patterning is achieved by placing a relief-patterned polydimethylsiloxane (PDMS) stamp in contact with an organic film and peeling off the stamp (Figure 1a). The procedure is done without applied pressure or heat and can be done in an ambient environment, although a nitrogen environment is preferred for organic light-emitting device (OLED) fabrication. This technique is applied to pattern 13 micron-sized features of a two-color OLED structure.



To fabricate a two-colored OLED, a hole-blocking or emissive layer is patterned using this technique. The in-plane roughness of the patterned feature is shown in the height image of a patterned stripe (Figure 1b) and a profile of the patterned feature is shown (Figure 1c). Electroluminescence (EL) from blue-green device with 13-micron-sized features is shown (Figure 2a), and EL from blue-red devices of 25-micron-sized features is shown (Figure 2b). This technique can be applied twice to pattern blue-red devices with finer features (Figure 2c, d).

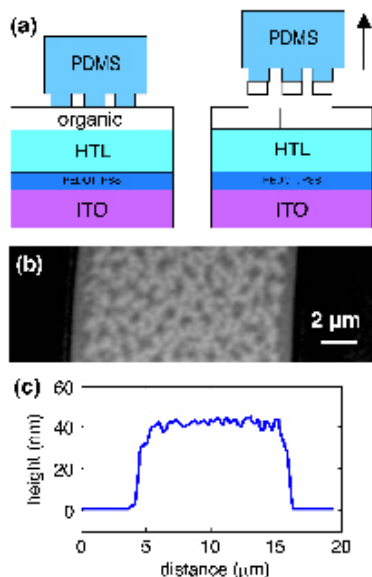


**Figure 1:** (a) Demonstration of the subtractive stamping technique. Placing PDMS stamp to the substrate and subsequent release lifts off organic thin film from substrate surface. (b) Top view of in-plane patterned 20-nm TAZ on 50-nm TPD / PEDOT:PSS / ITO / glass substrate from AFM. (c) AFM height data to view lift-off patterned region.

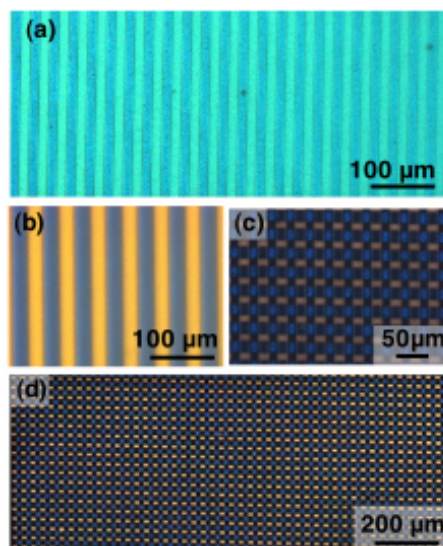


**Figure 2:** (a) EL of green-blue OLED from patterned hole-blocking layer for AIQ<sub>3</sub> (green) or TPD (blue) emission. (b) EL of red-blue OLED from a patterned emissive layer DCM<sub>2</sub>:AIQ<sub>3</sub> (red) or TPD (blue) emission and EL from red-blue patterned OLED by stamping twice to define finer features in (c) with a zoomed-out version (d).

## 7. Modeling of Electronic and Excitonic Processes in Quantum Dot LEDs

### Sponsors

ISN, MIT NSF MRSEC, PECASE

### Project Staff

P.O. Anikeeva, C.F. Madigan, J.E. Halpert, M.G. Bawendi, V. Bulović

Hybrid light-emitting devices (LEDs), consisting of organic charge transporting layers and colloidal quantum-dot (QD) emissive layers [1], exhibit narrow electroluminescence (EL) spectra, characteristic of colloidal QD luminescence. The manifested saturated color emission is particularly desirable in flat-panel display applications and is broadly applicable to other technologies requiring high spectral quality lighting. The development of novel QD deposition techniques such as microcontact printing [2] allowed us to experimentally investigate the mechanisms of QD-LED operation by varying the position of the emitting QD monolayer within the stacked organic structure. We find that imbedding the emissive QD monolayer into the hole-transporting layer <10 nm away from the interface between hole and electron-transporting layers, improves the quantum efficiency of the device by >50%, while maintaining QD-LED spectral purity (Figure

1). These findings and additional experiments led us to the conclusion that maximizing exciton generation on organic molecules and subsequent energy transfer to QDs, while minimizing QD charging with electrons, improves QD-LED performance.

In order to verify our conclusions based on the previous experimental observations, we built a theoretical model for charge and exciton transport in organic LEDs (OLEDs) and QD-LEDs. Considering carrier drift and diffusion, we numerically simulate carrier concentration and electric field profiles in device structures; based on them, we calculate exciton concentration profiles (Figure 2). We find that the results of our model are in qualitative agreement with experimental data. We find that exciton diffusion and non-radiative energy transfer from organic thin films to QDs lead to maximum exciton concentration on QD sites, resulting in QD-LED spectra dominated by QD emission. We find that imbedding QDs into the TPD hole-transporting layer reduces electron concentration at QD sites and consequently eliminates QD luminescence quenching. It also reduces the electric field across the QDs, eliminating exciton dissociation.

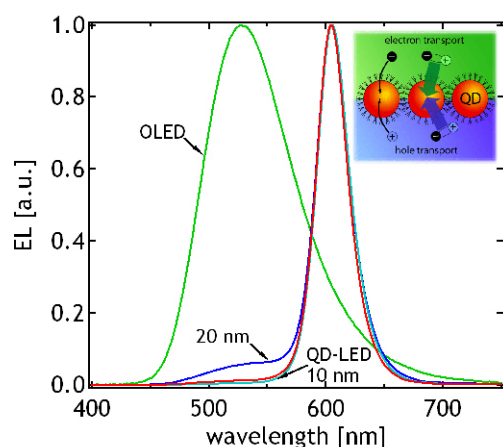


**Figure 1:** Normalized EL spectra of OLED, QD-LEDs with QDs at the TPD/Alq<sub>3</sub> interface, QDs imbedded into TPD 10 nm and 20 nm below the interface. Inset: Schematic diagram of the charge injection and energy transfer from organic charge transporting layers to a monolayer of colloidal QDs.

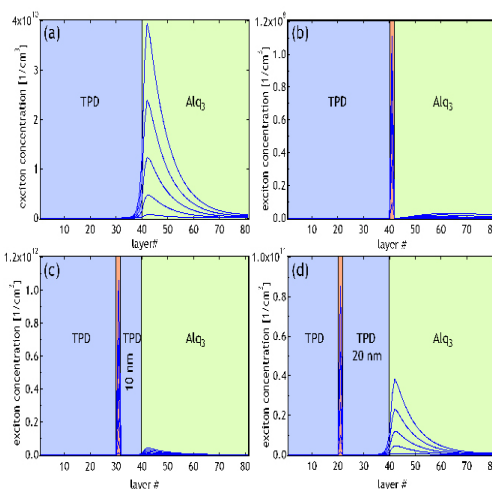


**Figure 2:** Exciton concentration profiles obtained from numerical simulations. (a) OLED, (b) QD-LED with QDs at the TPD/Alq<sub>3</sub> interface, (c) and (d) QDs imbedded into TPD 10 nm and 20 nm away from the interface. Theoretical exciton profiles are in qualitative agreement with experimental EL spectra shown in Figure 1.

## References

- [1] S.A. Coe-Sullivan, "Hybrid organic/quantum dot thin film structures and devices," Ph.D. thesis, Massachusetts Institute of Technology, Cambridge, 2005.
- [2] L. Kim, "Deposition of colloidal quantum dots by microcontact printing for LED display technology," M.Eng. thesis, Massachusetts Institute of Technology, Cambridge, 2006.

## 8. Heterojunction Photovoltaics Using Printed Colloidal Quantum Dots as the Photosensitive Layer

### Sponsors

ISN

### Project Staff

A.C. Arango, D.C. Oertel, M.G. Bawendi, V. Bulović

Colloidal quantum dot (QD) systems offer distinct optical and electronic properties that are not easily attained by other nanostructured semiconductors, such as highly saturated emission in QD light-emitting diodes, access to infrared radiation in QD photodetectors, and the prospect of optically optimized solar cell structures [1]. The prevailing deposition method for colloidal QD systems is spin casting, which introduces limitations such as solvent incompatibility with underlying films and the inability to pattern side-by-side pixels for multispectral photodetector arrays. In the present work we employ a non-destructive microcontact printing method, which allows for deposition of a thin quantum dot films onto a wide-band-gap organic hole transport layer, N,N'-Bis (3-methylphenyl)-N,N'-bis-(phenyl)-9,9-spiro-bifluorene (spiro-TPD), thus producing an inorganic/organic heterojunction that serves to enhance charge separation in the device. The top and bottom contacts are provided by ITO electrodes, allowing for near-transparency.

The performance of nanostructured devices is often critically dependent on the morphology of the constituent films in the device. Deposition of thin QD films from solution can result in rough and incomplete layers if the surface energy of the solvent is not well matched with the surface energy of the substrate. For instance, the low surface energy of a polydimethylsiloxane (PDMS) printing stamp must be modified to match the higher surface energy of the QD solvent in order to print smooth and complete QD films. When a layer of parylene-C is deposited on the PDMS stamp, a smooth and complete QD film can be printed, unlike the process in which a film is printed from a bare PDMS stamp (Figure 1). The device with a smooth and complete film yields superior performance, achieving a built-in potential ( $V_{bi}$ ) of 1.46V for a QD band gap of 1.97eV (Figure 2). The  $V_{bi}$  is 74% of the band gap, one of the highest values achieved for photovoltaics of any kind. The present focus is on improving the device's performance and optimizing the photodetection response in the 1- $\mu\text{m}$  to 2- $\mu\text{m}$  wavelength region by utilizing different QD film chemistries.

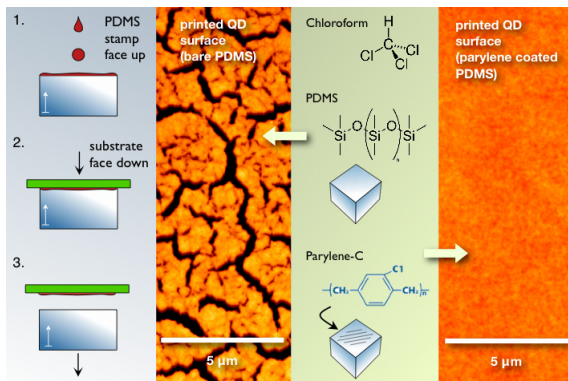


**Figure 1:** Printing process (far left) and AFM images of QDs deposited from bare PDMS (left) and parylene coated PDMS (right). The QD solution is spin cast onto the PDMS stamp (1) and allowed to dry under vacuum for 30 minutes; then the substrate is placed on the stamp (2) and released (3). Chloroform has less of a surface energy mismatch with parylene than with PDMS, resulting in improved wetting. Smooth and continuous QD films are achieved down to a thickness of one monolayer.

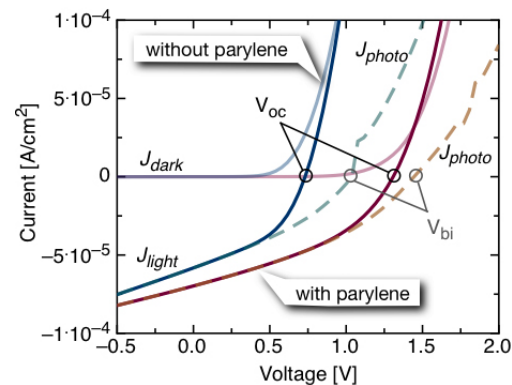


**Figure 2:** Current-voltage characteristics for a photovoltaic device consisting of a QD film printed from a bare PDMS stamp (blue) and a parylene coated PDMS stamp (red). The short circuit current and the open circuit voltage ( $V_{oc}$ ) are improved for the QD device deposited from parylene. The built-in potential ( $V_{bi}$ ) (the potential at which the current in light,  $J_{light}$ , is equal and opposite to the current in dark,  $J_{dark}$ ) reaches 1.46V.

### Reference

[1] D.C. Oertel, M.G. Bawendi, A.C. Arango, and V. Bulović, "Photodetectors based on treated CdSe quantum-dot films," *Applied Physics Letters*, vol. 87, no. 21, p. 213505, Nov 2005.

## 9. Organic/Quantum-dot Photoconductor

### Sponsors

ISN, CMSE

### Project Staff

T. Osedach, J. Ho, A. Arango, S. Geyer, M. Bawendi, V. Bulović

We demonstrate an organic/quantum-dot (QD) photodetector in which charge transport is governed by a single organic layer and the optical absorption can be tuned according to quantum confinement of QDs composing a second layer. The optical and electrical characteristics of the device can be optimized independently through the modification of these two layers. A similar device composed of organic materials was previously demonstrated by our group [1]. Our work stands in contrast to the operation of conventional layered organic photodetectors in which carriers generated at a dissociating interface must travel through both heterojunction materials to reach the opposite electrodes. In such a device both layers are crucial to charge transport, making it difficult to modify the optical properties of the device, such as absorption spectrum, without significantly affecting its electrical characteristics.

The device consists of metallic interdigitated electrodes over which an organic charge transport layer is thermally evaporated (see Figure 1). Microcontact printing is then used to deposit a 50-nm-thick layer of colloidal QDs, completing the structure. The organic/QD interface manifests a type-II heterojunction suitable for dissociating excitons. Under illumination, light is absorbed throughout both layers of the device. Excitons created within an exciton diffusion length of the heterojunction interface are dissociated there, increasing in the carrier concentrations of both layers. A bias corresponding to a field of  $\sim 104$  V/cm is applied across the electrodes to facilitate carrier collection. The increased hole density increases the organic film conductivity, which in turn manifests an increase in lateral current through the device. Figure 2 shows spectra of the external quantum efficiency exhibiting high efficiencies attributable to quantum-dot absorption. The device clearly separates the photogeneration and charge transport mechanisms and as such serves as a unique platform for studies of charge transfer at organic/QD interfaces for QD-sensitized photoactive devices.

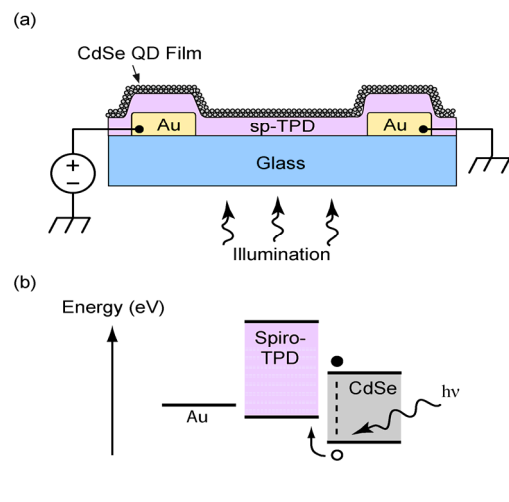


**Figure 1:** (a) Schematic of the device structure. (b) Energy band diagram. Excitons dissociate at the interface between the organic film and the quantum dots.

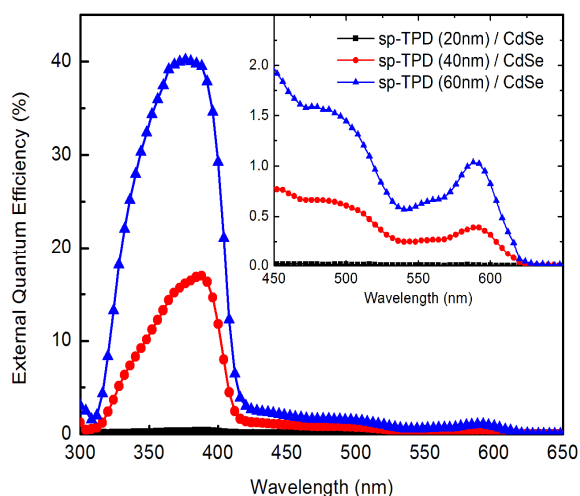


**Figure 2:** External quantum efficiency spectrum. High efficiencies have been measured at absorption peaks corresponding to the organic layer as well as to the quantum-dot layer.

### Reference

[1] J. Ho, A. Arango, and V. Bulović, "Lateral organic bi-layer heterojunction photoconductors," *Applied Physics Letters*, to be published.

## 10. Organic Multi-layer Lateral Heterojunction Phototransistors

### Sponsors

ISN, CMSE

### Project Staff

J.C. Ho, J.A. Rowehl, V. Bulović

We fabricate a two-terminal, lateral multi-layer phototransistor consisting of three molecular organic thin films with cascading energy bands (see Figure 1a): the charge transport layer is (CTL), N,N'-bis(3-methylphenyl)-N,N'-diphenyl-1,1'-biphenyl-4,4'-diamine (TPD); the charge spacer layer (CSL), tris(8-hydroxyquinoline)aluminum(III) (Alq<sub>3</sub>); and the exciton generation layer (EGL), 3,4,9,10-perylenetetracarboxylic bis-benzimidazole (PTCBI). Placing an interstitial spacer layer between the CTL and the EGL improves the external quantum efficiency of tri-layer phototransistors over bi-layer, Type-II heterojunction phototransistors.

Light excitation acts as a pseudo “gate electrode” by generating excitons in PTCBI (EGL). Those excitons diffuse to the PTCBI/Alq<sub>3</sub> interface where they dissociate, leaving the electron behind in PTCBI, while the hole is initially injected into Alq<sub>3</sub> from where it can transfer to the more energetically favorable states in TPD. Excess holes in the TPD film raise the hole carrier concentration in the TPD film and increase the device conductance by forming a channel of excess carriers at the TPD/Alq<sub>3</sub> interface. The thin film of Alq<sub>3</sub> (CSL), between TPD (CTL) and PTCBI (EGL), spatially separates the dissociated carriers, reducing the likelihood of bimolecular recombination across the TPD/PTCBI interface. Bi-layer heterojunction phototransistors consisting of TPD and PTCBI alone have been shown to improve the external quantum efficiency over single layers of TPD and PTCBI by several orders of magnitude [2]. By introducing a CSL in a lateral tri-layer arrangement, we demonstrate an order of magnitude improvement over bi-layer lateral phototransistors without a CSL (see Figure 1b). The phototransistor contacts consist of interdigitated gold fingers that form a 30- $\mu$ m-wide, 10- $\mu$ m-long serpentine channel. Measurement of the photocurrent from a biased multi-layer, lateral heterojunction device [Au/TPD(47.5  $\pm$  2) nm/Alq<sub>3</sub>(6.2  $\pm$  2) nm/PTCBI(52.5  $\pm$  2) nm] reveals an internal quantum efficiency of (16  $\pm$  1)% at an optical excitation wavelength of 573 nm. A thickness study of the Alq<sub>3</sub> spacer layer experimentally demonstrates the dependence of the carrier lifetime (at a heterointerface) and photoresponse efficiency on the spatial separation of dissociated charge.

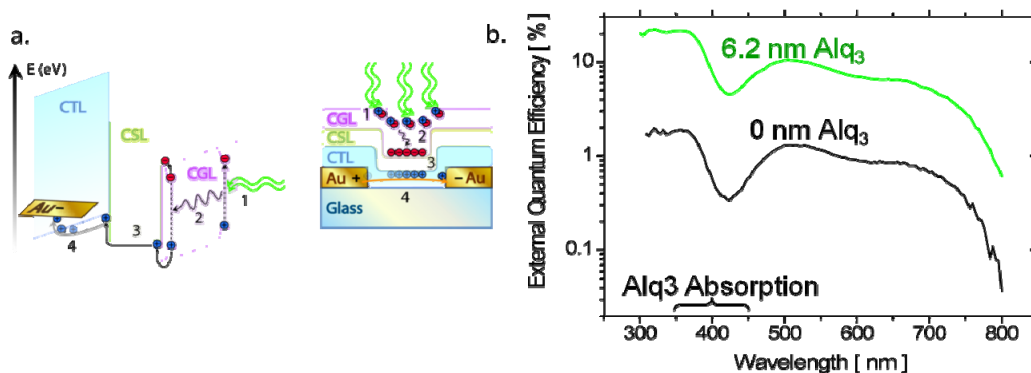


**Figure 1:** a. Energy band/cross-sectional diagrams of tri-layer phototransistors (1. absorption, 2. exciton diffusion, 3. exciton dissociation, 4. charge transport) b. Spectral response of EQE showing benefit of CSL.

### References

[1] J. Ho, J. Rowehl, and V. Bulović, “Organic multi-layer lateral heterojunction phototransistors,” to be presented at *Electronic Materials Conference*, Santa Barbara, CA, June 2008.

[2] J. Ho, A. Arango, and V. Bulović, "Lateral organic bi-layer heterojunction photoconductors," *Applied Physics Letters*, June 2008, to be published.

### 11. Organic Thin-film Transistor Integrated Circuits

#### Sponsors

SRC/FCRP C2S2, Hewlett-Packard, NSERC Fellowship

#### Project Staff

D. He, I. Nausieda, K. Ryu, A.I. Akinwande, V. Bulović, C.G. Sadini

The organic thin-film transistor (OTFT) is a field-effect transistor technology that uses an organic material as the semiconductor. Electronically, OTFTs have field-effect mobilities that are comparable to those of hydrogenated amorphous silicon TFTs [1]. Mechanically, organic materials can be processed at room temperature, thus permitting substrates that are low-cost, large-area, and mechanically flexible [2]. We investigate the OTFT technology through device characterization and circuit design.

The OTFTs used in our work are lithographically processed at temperatures less than 95 °C to produce integrated circuits compatible with mechanically-flexible substrates [3]. Figure 1a shows the OTFT device cross-section, with typical output characteristics in Figure 1b. Device parameters such as threshold voltage, charge mobility, subthreshold slope, and contact resistance are characterized and studied.

We design OTFT circuits to achieve two goals: to aid the understanding of device physics and to evaluate the feasibilities of various OTFT applications. One such circuit is the complementary-to-absolute-temperature (CTAT) circuit shown in Figure 2. The CTAT circuit promotes the study of thermally activated device mechanisms. At the same time, we use the circuit to explore highly-linear and low-power temperature-sensing applications. Another OTFT circuit is the 4×4 active-matrix imager, as described in [4]. Additional OTFT circuits include digital logic gates, ring oscillators, display pixel drivers, comparators, and static random-access memory cells.

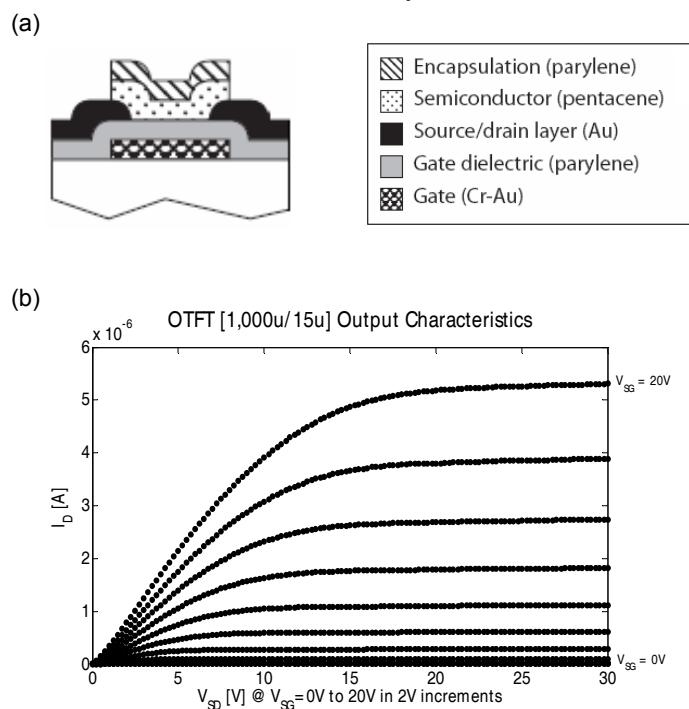


**Figure 1:** (a) OTFT device cross-section and (b) typical OTFT output characteristics.

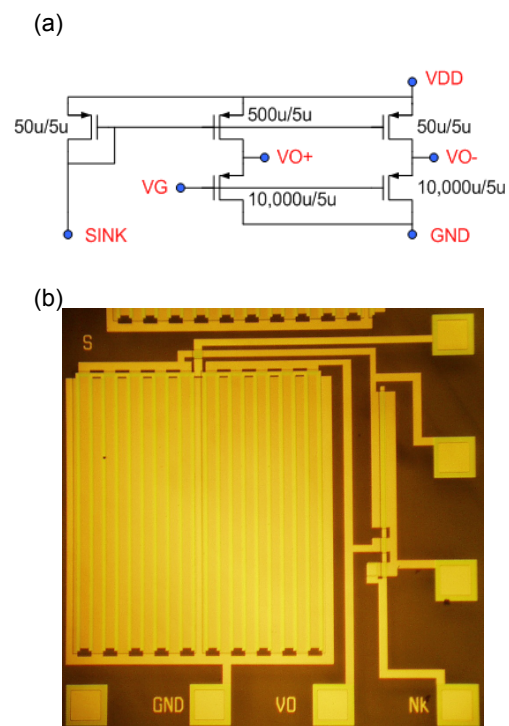


**Figure 2:** (a) CTAT circuit schematic and (b) its die micrograph (area of  $1\text{mm}^2$ ).

## References

- [1] Y.Y. Lin, D.J. Gundlach, and T.N. Jackson, "High-mobility pentacene organic thin film transistors," *Device Research Conference Digest*, June 1996, pp. 80–81.
- [2] M. Chason, P.W. Brazis, J. Zhang, K. Kalyanasundaram, and D.R. Gamota, "Printed Organic Semiconducting Devices," *Proc. of the IEEE*, July 2005, pp. 1348–1356.
- [3] I. Kymissis, C.G. Sodini, A.I. Akinwande, and V. Bulovic, "An organic semiconductor based process for photodetecting applications," *IEEE International Electron Devices Meeting Technical Digest*, Dec. 2004, pp. 377–380.
- [4] I. Nausieda, K. Ryu, I. Kymissis, A.I. Akinwande, V. Bulovic, and C.G. Sodini, "An organic imager for flexible large area electronics," *Digest of IEEE International Solid-State Circuits Conference*, San Francisco, Feb. 2007, pp. 72–73.

## 12. Lithographically Patterned Metal Oxide Transistors for Large-area Electronics

### Sponsors

Hewlett-Packard, DARPA

### Project Staff

A. Wang, B. Yaglioglu, H. Tang, C.G. Sodini, V. Bulović, A.I. Akinwande

Recently, sputtered metal-oxide-based field-effect transistors (FETs) have been demonstrated with higher charge carrier mobilities, higher current densities, and faster response performance than amorphous silicon FETs, which are the dominant technology used in display backplanes [1-3]. Because the optically transparent semiconducting oxide films can be deposited at near-room temperatures, these materials are compatible with future generations of large-area electronics technologies that require flexible substrates [4]. It is possible to process FETs by shadow-mask patterning, but this method limits the range of feature sizes, accuracy of pattern alignment, and scalability of the process to large substrates. Consequently, our project aims to develop a low-temperature, lithographic process for metal oxide-based FETs that can be integrated into large-area electronic circuits.

We have fabricated top-gate, fully lithographic FETs of varying channel lengths on 100-mm glass wafers with a sputtered ZnO:In<sub>2</sub>O<sub>3</sub> channel layer, using an organic polymer, parylene, as the gate dielectric and indium-tin-oxide (ITO) for source/drain contacts. All layers were subtractively patterned by a combination of dry- and wet-etch processes. Figure 1 shows a micrograph of several completed FETs. Current-voltage characteristics for a single device (pictured in inset of Figure 1) appear in Figure 2. From the current-voltage and capacitance-voltage curves, device- and circuit parameters such as threshold voltage, subthreshold slope, gate leakage, and channel capacitance can be extracted and also used to monitor the reproducibility of our process. These measurements are used as a guide to determine processing conditions for the fabrication of oxide-based field-effect transistors and circuits.

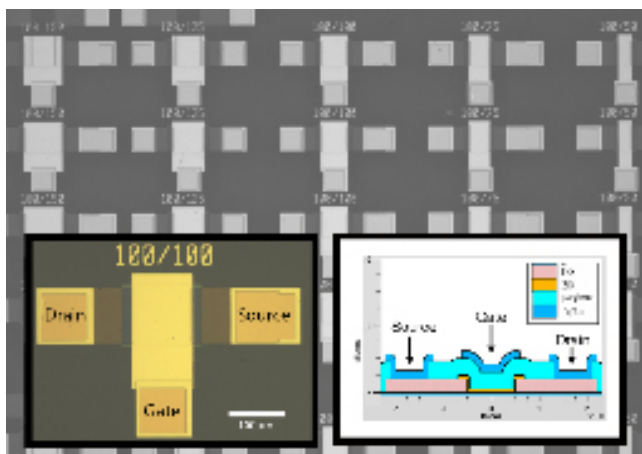


**Figure 1:** Micrograph of fabricated array of single devices with varying channel lengths. The left inset gives a larger view of a single field effect transistor ( $W/L = 100\mu\text{m} / 100\mu\text{m}$ ). The right inset shows a schematic cross-section of the device.

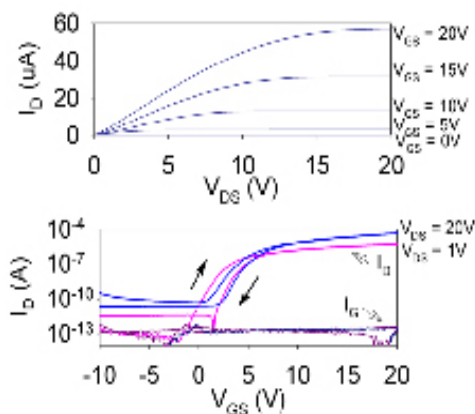


**Figure 2:** Electrical characteristics of lithographically patterned FET ( $W/L = 100\mu\text{m} / 100\mu\text{m}$ ). Output curves are plotted in the top graph; double-swept transfer curves taken in saturation and triode regions are plotted on the bottom. As the bottom graph shows, gate leakage current through the parylene dielectric is low.

## References

- [1] R.L. Hoffman, B.J. Norris, and J.F. Wager, "ZnO-based transparent thin-film transistors," *Applied Physics Letters*, vol. 82, no. 5, pp. 733-735, Feb. 2003.
- [2] P.F. Carcia, R.S. McLean, M.H. Reilly, and G. Nunes, "Transparent ZnO thin film transistors fabricated by RF magnetron sputtering," *Applied Physics Letters*, vol. 82, no. 7, pp. 1117-1119, Feb. 2003.
- [3] K. Nomura, H. Ohta, A. Takagi, T. Kamiya, M. Hirano, and H. Hosono, "Room-temperature fabrication of transparent flexible thin-film transistors using amorphous oxide semiconductors," *Nature*, vol. 432, pp. 488-492, Nov. 2004.
- [4] E. Fortunato, P. Barquinha, A. Pimentel, A. Goncalves, A. Marques, L. Pereira, and R. Martins, "Fully transparent ZnO thin-film transistor produced at room temperature," *Advanced Materials*, vol. 17, pp. 590-594, Mar. 2005.



### 13. Engineering the Flatband Voltage in Organic Field-effect Transistors for Enhancement-depletion Mode Logic

#### Sponsors

SRC/FCRP C2S2

#### Project Staff

I. Nausieda, D. He, K. Ryu, A.I. Akinwande, V. Bulović, C.G. Sodini

Organic semiconductors could enable large-area, mechanically flexible electronic systems such as e-paper, large-area imagers, and roll-able displays due to their low processing temperatures and suitable electronic properties. We have developed a near-room-temperature ( $\leq 95$  °C), scalable process to fabricate integrated organic field-effect transistors (OFETs) [1].

The OFET's semiconducting layer is a thin (15-nm) film of pentacene - chosen for its air-stability and high hole mobility ( $\approx 1$  cm<sup>2</sup>/Vs) [2]. Since there exists no air-stable, electron-transporting organic semiconductor with comparable mobility, our process produces p-channel transistors only. The nominal process pictured in Figure 1 yields enhancement-mode OFETs with threshold voltages of -1V.

The goal of this project is to achieve enhancement and depletion mode devices on a single substrate. The OFET flatband voltage, nominally the difference between the gate and semiconductor work functions, may be shifted by changing the gate metal work function. With the use of two gate metals, enhancement and depletion mode devices can be obtained. Such a process would enable the creation of high-noise margin inverters, robust to process variation (see Figure 2). Connecting the gate to the source permits use of the depletion-mode transistors as current sources, making possible a variety of analog circuits such as high-gain amplifiers and comparators.

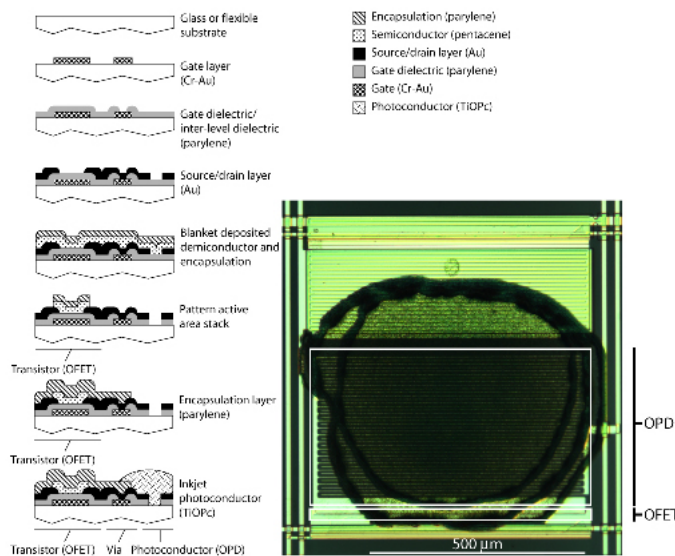


**Figure 1:** Integrated process for OFETs and organic photoconductors (OPDs) developed at MIT.

#### References

- [1] I. Nausieda, K. Ryu, I. Kymissis, A.I. Akinwande, V. Bulović, and C.G. Sodini, "An organic active-matrix imager," *IEEE Transactions on Electron Devices*, vol. 55, no. 2, pp. 527-532, Feb. 2008.  
 [2] H. Klauk et al., "High-mobility polymer gate dielectric pentacene thin film transistors," *Journal of Applied Physics*, vol. 92, no. 9, pp. 5259-5263, Nov. 2002.

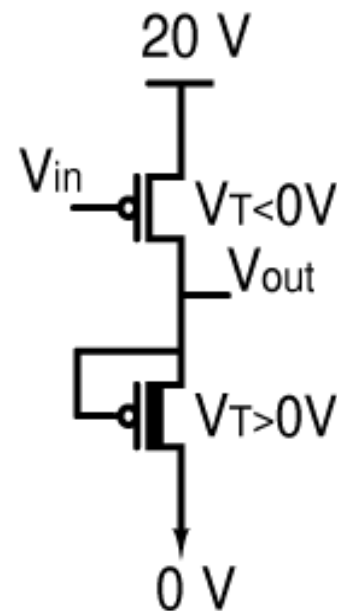


**Figure 2:** Inverter/common-source amplifier with enhancement-mode driver and depletion-mode load.

## 14. Bias-induced Instability in Pentacene and Zinc Oxide Thin-film Transistors

### Sponsors

SRC/FCRP C2S2

### Project Staff

K. Ryu, D. He, I. Nausieda, A. Wang, A.I. Akinwande, V. Bulović, C.G. Sodini

Thin-film transistors (TFTs) are a type of field-effect transistor made by depositing a thin film of semiconductor as the active layer over a substrate that provides mechanical support. This thin semiconductor layer is polycrystalline or amorphous, which results in trap states in the bandgap and therefore exhibits poorer carrier mobility than single crystal films. However, TFTs can enable large-area electronics because they are not limited by the substrate materials. The TFTs based on semiconducting organic small molecules (e.g., pentacene) and metal oxides (e.g., zinc oxide) offer near-room-temperature processing, which makes them compatible with lightweight, flexible plastic substrates. These new devices have been employed to make paper-like flexible displays that are commercially available. Although TFTs' primary function has been limited to the switching elements in displays, there is significant interest in expanding their function to integrate new digital and analog circuit blocks such as display decoders, multiplexers, and OLED drivers. Operational stability is required for these new applications, but both organic TFTs and metal oxide TFTs have been reported to have bias-stress stability problems. Figures 1 and 2 show that for gate bias stress of -30V for ten seconds, the flatband voltage shifts 0.6 V.

The goal of this work is to investigate the mechanisms that cause bias-induced instability in pentacene and zinc oxide transistors and use the knowledge to develop a method of quenching bias-instability for thin-film transistors at low processing temperatures. The work involves physical modeling of I-V, and C-V characteristics of TFTs to identify the changing physical parameters. Electrical characterization methods such as  $1/f$  noise, I-V, and C-V measurements will be employed to determine the mechanisms that cause bias instability.

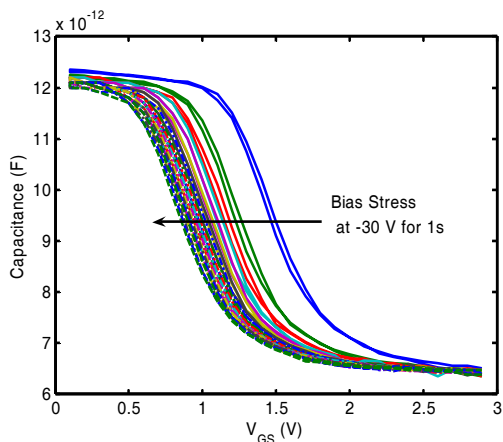


**Figure 1:** A C-V graph of a pentacene TFT (1000/25  $\mu\text{m}$ ), which shows  $V_{\text{FB}}$  shift as the bias-stress is applied.

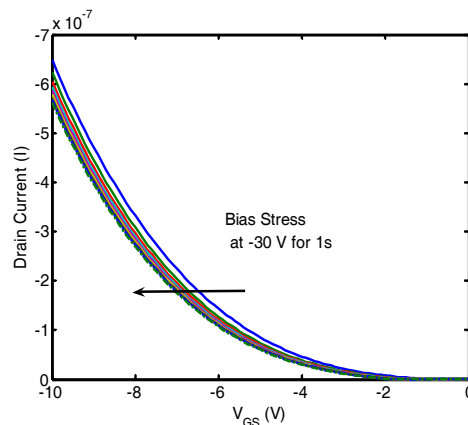


**Figure 2:** An I-V graph of a pentacene TFT (1000/25  $\mu\text{m}$ ), which shows  $V_{\text{FB}}$  shift as the bias-stress is applied.

### References

- [1] K. Ryu, I. Kymissis, V. Bulović, and C.G. Sodini, "Direct extraction of mobility in pentacene OFETs using C-V and I-V measurements," *IEEE Electron Device Letters*, vol. 26, no. 10, pp. 716-718, Oct. 2005.
- [2] I. Nausieda, K. Ryu, I. Kymissis, A.I. Akinwande, V. Bulović, and C.G. Sodini, "An organic imager for flexible large area electronics," *IEEE International Solid-State Circuits Conference Digest*, San Francisco, Feb. 2007, pp. 72-73.

## 15. Inkjet Printing of P3HT/PCBM Solar Cells

### Sponsors

ISN, CMSE

### Project Staff

T. Osedach, A. Arango, J. Chen, V. Bulović

Polymeric solar cells offer the promise of a low-cost alternative to conventional inorganic photovoltaic devices. Particularly encouraging are solar cells consisting of blends of the polymer poly(3-hexylthiophene) (P3HT) and the fullerene derivative [6,6]-phenyl-C61-butyric acid methyl ester (PCBM) sandwiched between electrodes (see Figure 1). Recently, power efficiencies as high as 5.2% have been reported [1]. In an attempt to further improve the performance and cost-effectiveness of these solar cells so that they may become a more viable technology, we are exploring a number of variations to the standard processing procedure to fabricate them.

Presently, the processing of P3HT:PCBM devices used by most other groups involves a combination of spin-coating and thermal evaporation steps that are limited to small substrate sizes. In our study, we have used inkjet printing, a low-cost and highly scalable deposition technique, to deposit the active layers in P3HT:PCBM solar cells. The deposition of metal electrodes with inkjet printing is also currently being explored. Figure 2 shows current-voltage characteristics of a printed solar and a control device with a spin-coated active layer. The short-circuit current of the printed solar cell in this case exceeds that of the control device.

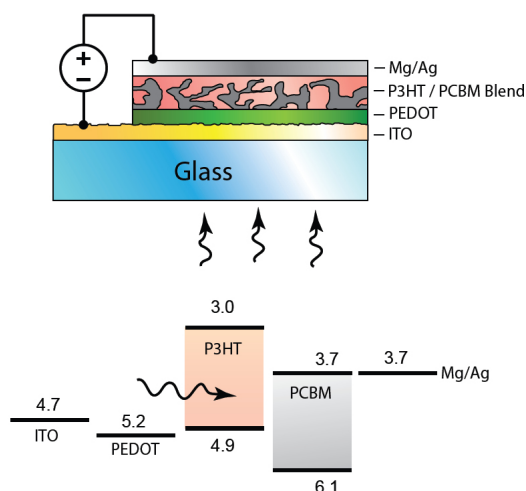


**Figure 1:** (top) Device structure of a P3HT:PCBM solar cell. (bottom) Energy band diagram of the device. The P3HT and PCBM create a type-II heterojunction suitable for separating excitons.

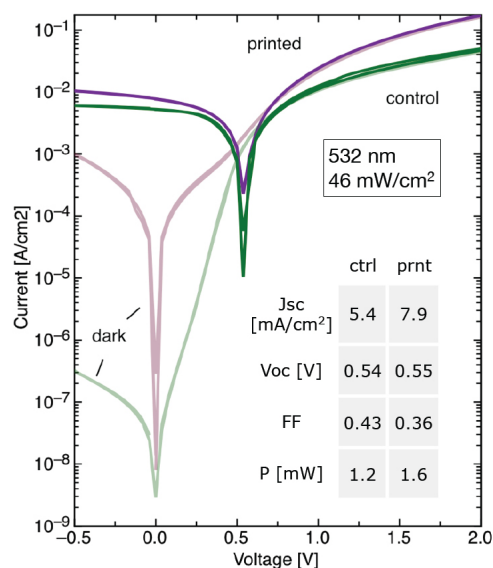


**Figure 2:** Current-voltage characteristics of an inkjet-printed solar cell versus a control device fabricated using spin-casting. The printed device exhibits a superior short-circuit current and open-circuit voltage, but a higher dark current.

### Reference

[1] M.D. Irwin, D.B. Buchholz, A.W. Hains, R.P.H. Chang, and T.J. Marks, "P-type semiconducting nickel oxide as an efficiency-enhancing anode interfacial layer in polymer bulk-heterojunction solar cells," *Proc. National Academy of Sciences*, vol. 105, pp. 2783-2787, 2008.

## Publications

### Journal Articles, Published

J.R. Tischler, M. S. Bradley, Q. Zhang, T. Atay, A. Nurmikko, V. Bulović, "Solid State Cavity QED: Strong Coupling in Organic Thin Films," *Organic Electronics* **8**, 94-113 (2007).

H. Huang, A. Dorn, V. Bulović, M.G. Bawendi, "Electrically Driven Light Emission from Single Colloidal Quantum Dots at Room Temperature," *Applied Physics Letters* **90**, 023110 (2007).

C. Madigan and V. Bulović, "Exciton Energy Disorder in Polar Amorphous Organic Thin Films: Monte Carlo Calculations," *Physical Review B* **75**, 081403(R) (2007).

V. Leblanc, J.L. Chen, S.H. Kang, V. Bulović, M.A. Schmidt, "Micromachined printheads for the evaporative patterning of organic materials and metals," *Journal of Microelectromechanical Systems* **16** 394-400 (2007).

P.O. Anikeeva, J.E. Halpert, M.G. Bawendi, V. Bulović, "Electroluminescence from a mixed red-green-blue colloidal quantum dot monolayer," *Nano Letters* **7**, 2196-2200 (2007).

H. Huang, A. Dorn, G.P. Nair, V. Bulović, M.G. Bawendi, "Bias-Induced Photoluminescence Quenching of Single Colloidal Quantum Dots Embedded in Organic Semiconductors," *Nano Letters* **7**, 3781-3786 (2007).

J. Yu and V. Bulović, "Micropatterning metal electrode of organic light emitting devices using rapid polydimethylsiloxane lift-off," *Applied Physics Letters* **91**, 043102 (2007).

Q. Zhang, T. Atay, J.R. Tischler, M.S. Bradley, V. Bulović, A.V. Nurmikko, "Highly efficient resonant coupling of optical excitations in hybrid organic/inorganic semiconductor nanostructures," *Nature Nanotechnology* **2**, 555-559 (2007).

J.L. Chen, V. Leblanc, S.H. Kang, P.J. Benning, D. Schut, M.A. Baldo, M.A. Schmidt, V. Bulović, "High definition digital fabrication of active organic devices by molecular jet printing," *Advanced Functional Materials* **17**, 2722-2727 (2007).

C. Madigan, E. Howe, V. Bulović, P. Mardilović, P. Kornilovitch, "Planarization in electrochemically fabricated nanodimensional films," *Journal of Physical Chemistry C*, **112**, 7318-7325 (2008).

I. Nausieda, K. Ryu, I. Kymissis, A. Akinwande, V. Bulović, C.G. Sodini, "An Organic Active-Matrix Imager," *IEEE Transactions on Electron Devices*, **55**, 527-532 (2008).

J.M. Caruge, J.E. Halpert, V. Wood, V. Bulović, and M.G. Bawendi, "Colloidal Quantum-Dot Light-Emitting Diodes with Metal-Oxide Charge Transport Layers," *Nature Photonics* **2**, 247-250, 4 pages (2008).

Yu, J. and V. Bulović, "Using Integrated Optical Feedback to Counter Pixel Aging and Stabilize Light Output of Organic LED Display Technology," *IEEE Journal of Display Technology* (2008).

Ho, J., A. Arango, and V. Bulović, "Lateral Organic Bi-layer Heterojunction Photoconductors," *Applied Physics Letters* (2008).

### Theses

#### Ph.D. Thesis:

Tischler, Jonathan, "Solid State Cavity QED: Practical Applications of the Strong Coupling Limit," June 2007 (EECS).

Chen, (Gerry) Jianglong, "Novel Patterning Techniques for Manufacturing Organic and Nanostructured Electronics," June 2007 (DMSE).

**M.Eng. Thesis:**

Shirasaki, Yasuhiro, "Efficient Förster Energy Transfer From Phosphorescent Organic Molecules to J-aggregate Thin Film," February 2008 (EECS).

Abdu, Hassen, "Molecular and Quantum Dot Floating Gate Non-Volatile Memories," June 2008 (EECS).  
Friend, David, "Theory and Fabrication of Evanescently-Coupled Photoluminescent Devices," June 2008 (EECS)

Tang, Hui, "Near Room Temperature Lithographically Processed Metal-Oxide Transistors," June 2008 (EECS).

